Polymer Journal (2017) 49, 789–798
© 2017 The Society of Polymer Science, Japan (SPSJ) All rights reserved 0032-3896/17
www.nature.com/pj

ORIGINAL ARTICLE

Membranes based on carboxymethyl chitin as potential scaffolds for corneal endothelial transplantation

Wenhua Xu[1,3], Zheying Wang[1,3], Tong Li[1], Liping Wang[2], Wenhua Zhang[1], Ye Liang[2] and Chengyu Liu[1]

To overcome the worldwide shortage of donor corneas, transplantation of cultured corneal endothelial cells (CECs) as substitutes has been attempted in experimental studies to treat corneal endothelial dysfunction. In the present study, corneal endothelial scaffolds were prepared using carboxymethyl chitin (CMCT) or carboxymethyl chitosan (CMCTS) as the main ingredient and gelatin (gel) at a mass ratio of 20:1. The transmittances of the membranes were examined at different wavelengths (400, 500, 600, 700 and 800 nm). The cytotoxicity of the blend membranes was evaluated by MTT (3-(4,5-dimethylthiazol-2yl)-2,5-diphenyltetrazolium bromide) assay. The properties of both membranes, including biodegradability, immunogenicity and toxicity, were determined by implantation experiments in Sprague-Dawley rats. Then the rabbit primary CECs were implanted onto the blended membranes to evaluate their cytocompatibility. Results indicated that both the CMCT/gel and CMCTS/gel blended membranes exhibited good transparency and cytocompatibility, with relatively low *in vivo* toxicity. However, the CMCT/gel membranes showed a higher degradation rate and milder immune response *in vivo* compared with the CMCTS/gel. The degradation time of the CMCT/gel membranes was <8 weeks in the subcutaneous tissues and 4 weeks in the skeletal muscles. Thus the CMCT/gel blended membrane could be a more promising candidate for constructing endothelial scaffold in corneal replacement.
Polymer Journal (2017) **49,** 789–798; doi:10.1038/pj.2017.50; published online 13 September 2017

INTRODUCTION

The corneal endothelium is a monolayer between the corneal stroma and the aqueous humor, which maintains corneal transparency via a pump and barrier function. Any damage to the corneal endothelium caused by pathological factors, such as Fuchs endothelial corneal dystrophy, surgical trauma, and burns, cause severe vision loss.[1] Unlike other cell types, corneal endothelial cells (CECs) close the wound gap mostly by cell migration and dissemination because of their limited proliferative ability.[2] Consequently, corneal transplantation is the sole therapeutic choice for treating corneal endothelial dysfunction.[3] However, approximately 53% of the world's population has no access to corneal transplantation.[4] To overcome the worldwide shortage of donor corneas, transplantation of CEC-cultured scaffolds has been attempted in experimental studies as a substitute for corneal replacement.[5–8]

Chitin is the second-most abundant biopolymer in nature and is extracted from crustacean shells and the fungi cell walls. Chitosan is an alkaline deacetylated product of chitin. Studies have shown that chitin and chitosan are good biomaterials with unique physicochemical and biological properties, such as biocompatibility, biodegradability, non-toxicity, antimicrobial activity and accessibility, and is inexpensive.[9–11] However, applications of chitin and chitosan have been limited because of their insolubility in water and most common organic solvents. Various chemical modifications have been performed to broaden the applicability of these polymers.[12] Among these, the carboxymethyl chitin (CMCT) and carboxymethyl chitosan (CMCTS) derivatives have increased water solubility,[11] high moisture retention ability,[13] enhanced biocompatibility,[14] better biodegradability, nontoxicity[15] and the ability to promote cell adhesion compared with those of their precursors. Several studies have focused on the use of CMCTS or CMCT composites in bone, cartilage, vessel and tooth tissue engineering.[16–18] However, research on the biomedical utilization of CMCTS- and CMCT-based materials as corneal endothelium scaffolds are limited.[19] Furthermore, studies on the differences in the properties of these two biomaterials are lacking. In addition, research on chitin and its derivatives as biomaterials is lagging behind that of chitosan.[20] However, chitin and its derivatives have significant and inherently favorable material and chemical properties. Therefore, in the present study, CEC scaffolds prepared with CMCT and CMCTS were constructed and their properties were compared to determine the suitability of either material as carrier of CECs.

[1]College of Medicine, Qingdao University, Qingdao, China and [2]Key Laboratory, Department of Urology and Andrology, The Affiliated Hospital of Qingdao University, Qingdao, China
[3]These authors contributed equally to this work.
Correspondence: Dr Y Liang, Key Laboratory, Department of Urology and Andrology, The Affiliated Hospital of Qingdao University, Qingdao, Shan Dong 266003, China.
E-mail: liangye82812@163.com
or Professor C Liu, College of Medicine, Qingdao University, Qingdao, Shan Dong 266003, China.
E-mail: qd_lchy@163.com
Received 23 March 2017; revised 29 June 2017; accepted 23 July 2017; published online 13 September 2017

In this study, corneal endothelial scaffolds were prepared with CMCT or CMCTS, blended with gelatin (gel) at the mass ratio of 20:1, based on our previous studies.[21] To evaluate and compare properties of the blended membranes for use in corneal transplantation, we examined their transparency, cytocompatibility, biodegradability, immunogenicity and toxicity. The results indicated that both the CMCT/gel and CMCTS/gel blended membranes exhibited good transparency and cytocompatibility, with relatively low *in vivo* toxicity. However, the CMCT/gel membranes degraded faster *in vivo* and induced milder immune responses compared with the CMCTS/gel membrane. Thus we suggest that the CMCT/gel blended membrane might be more suitable as an endothelial scaffold for CECs in corneal replacement.

MATERIALS AND METHODS

Materials and reagents

In this research, all animal procedures were performed in accordance with the ARVO Statement for the Use of Animals. Sprague-Dawley (SD) rats were purchased from Qingdao Laboratory Animal Center, Qingdao, China. New Zealand Rabbits were purchased from Agriculture Science Research Department of Shandong Province. The L929 cell line was provided by typical culture preservation commission cell bank, Chinese Academy of Sciences. CMCTS (the degree of deacetylation was 96%, and the average molecular weight was134 kDa) and CMCT (average molecular weight 115 kDa) were prepared in our laboratory. Gel, 1,4-butanediol diglycidyl ether (BDDGE) and 3-(4,5-dimethylthiazol-2yl)-2,5-diphenyltetrazolium bromide (MTT) were purchased from Sigma Chemical Co. (St Louis, MO, USA). Materials for cell culture, including Dulbecco's modified Eagle's medium (DMEM)/F12 culture medium, fetal bovine serum (FBS), trypsin, penicillin and streptomycin were purchased from Gibco Co. (Grand Island, NY, USA). Antibodies against leukocyte common antigen (LCA) was purchased from Bioss (Beijing, China). All other reagents used were of reagent grade.

Preparation of CMCTS and CMCT blended membranes

CMCTS or CMCT solution (2%) was mixed with 2% gel (weight ratio of polysaccharide: gel = 20:1) in tubes. 5% BDDGE ethanol solution was then added to the mixture as crosslinker (with volume ratio of 200:1). After stirring adequately, the mixtures were poured onto a flat glass and dried at 30 °C for 18 h to form thin membranes. The CMCTS or CMCT blended membranes were soaked with double-distilled water, and discs with a diameter of 6 or 11 mm were excised with a puncher.

Measurement of the transparency of the blended membranes

The optical transmittance of the membranes was examined by irradiating them with lights of different wavelengths (400, 500, 600, 700 and 800 nm) using a spectrophotometer (Thermo Multiskan Go Spectrum, Vantaa, Finland).

Cytotoxicity evaluation of the blend membranes

According to the evaluation standard of cytotoxicity (GB/T16886.5-2003),[22] the relative growth rate (RGR) of L929 cells in the blend membrane extraction was detected by MTT assay to evaluate the cell toxicity. The blend membrane was placed in the DMEM medium containing 10% FBS for 24 h at 37 °C. The superficial area of the membrane in the medium was 6 cm^2 ml^{-1}. Then L929 cells in logarithmic growth phase were digested in 3×10^4 cells ml^{-1} and inoculated into the 96-cell culture plate. After culture for 24 h at 37 °C/5% CO_2, medium of the experimental group was changed into the membrane extract. The cells cultured with fresh culture medium served as the control group. The growth of the cells was detected using MTT assay at 24 and 48 h. The optical density at 490 nm (OD_{490}) values were determined using a spectrophotometer (Thermo Multiskan Go Spectrum). Medium without cells was used as the blank group. The RGR (%) was calculated with the following formula: RGR (%) = $(OD_1-OD_0)/(OD_2-OD_0)\times100\%$, where OD_0, OD_1 and OD_2 were the average OD of the blank, experimental and negative control groups, respectively. Experiments were performed in quintuplicate.

The cytotoxicity scoring criteria are shown as follows: (1) Material with RGR > 100% grades 0 and is qualified; (2) Material with RGR ranging from 80% to 99% grades 1 and is similarly qualified; (3) Material with RGR ranging from 50% to 79% grades 2 and should be comprehensively evaluated with the cell morphology; (4) Material with RGR ranging from 30% to 49% grades 3 and is not qualified; and (5) Material with RGR < 29% grades 4 and is not qualified.

Evaluating in vivo histocompatibility and degradability

Surgery. The *in vivo* degradability and histocompatibility of the membranes were examined by implanting the blended membranes into the subcutaneous tissue and skeletal muscle of SD rats. The rats, weighing about 200 g, were kept under specific pathogen-free conditions throughout the experiment. The sterile CMCTS or CMCT blended membranes (6 mm in diameter) were embedded into both subcutaneous tissue and skeletal muscle of anesthetized rats. Rats implanted with 3-0 nonabsorbable surgical sutures served as the negative control. The rats of the sham operation group were operated but did not receive an implant.

General observation and hematoxylin–eosin (HE) staining of the implanted membranes. After surgery, at least three rats in each group were killed at 1, 2, 4 and 8 weeks after the implantation. At these time points, the membranes in the subcutaneous tissue were observed and photographed. The surgery sites in both the subcutaneous tissue and skeletal muscle were then removed. The samples of membranes and their surrounding tissues were fixed in 10% neutral-buffered formaldehyde for 24 h, dehydrated in a graded series of ethanol solutions, embedded in paraffin and stained with HE for histological observation.

Immumohistochemical staining. The samples (1 and 2 weeks after the surgery) embedded in paraffin were cut on a microtome at a thickness of 10 μm and blocked for 1 h in 10% normal goat serum in phosphate-buffered saline (PBS) containing 0.3% Triton X-100 and then incubated overnight at room temperature in primary antibodies diluted in 1% normal goat serum in PBS containing 0.3% Triton X-100. The sections were then incubated overnight (4 °C) in rabbit anti-LCA antibody (1:200, Bioss, Beijing, China) and then washed thrice for 10 min in PBS and then incubated in anti-rabbit immunoglobulin G (ZSZB Bio, Beijing, China) for 2 h. After several PBS washes, tissues were mounted onto slides and allowed to briefly dry before coverslipping.

Liver, kidney and spleen index and histological observation. The index of liver, kidneys and spleen of the killed animals were calculated using the following formula: Relative weight = W/W_0, where W was the weight of the liver, kidneys or spleen and W_0 was the body weight of the experimental animal. The samples of liver, kidneys and spleen of the killed animals at 8 weeks were also fixed in 10% neutral-buffered formaldehyde for 24 h, dehydrated in a graded series of ethanol solutions, embedded in paraffin and stained with HE for histological observation.

Membranes as potential scaffold for CECs

Rabbit CEC primary culture. CECs of young New Zealand rabbits (1-month old) were separated together with the Descemet's membrane and cultured with DMEM/F12 medium supplemented with 15% FBS using the tissue block method.[23] The cells were then cultured in a CO_2 (5%) incubator at 37 °C. After reaching 80% confluence, cells were used in subsequent experiments after one generation.

CEC culture on membranes and fluorescence microscope imaging. Sterile blended membranes (11 mm in diameter) were placed in the wells of 48-well cell culture plates. CECs were seeded onto the CMCTS or CMCT blended membranes at a density of 5.0×10^5 cells ml^{-1}. The control group comprised CEC-treated wells without membranes. Cells were cultured at 37 °C/5% CO_2. After culturing for 48 h, CECs seeded on the two kinds of scaffolds were washed by PBS and labeled with 5,6-carboxyfluorescein diacetate succinimidyl ester (CFSE). Cell morphology and attachment were monitored using light and fluorescence microscopy (CKX41SF, Olympus, Tokyo, Japan). On the third

day, growth of the cells was detected using the MTT assay. OD_{490} values were determined using a spectrophotometer (Thermo Multiskan Go Spectrum).

Scanning electron microscopy (SEM) of CECs cultured on scaffolds. CECs were seeded on the two types of membranes as described in the previous section. After culturing for 2 days, the CEC-cultured scaffolds were washed thrice with PBS and fixed in 2.5% glutaraldehyde for 4 h. Subsequently, the samples were dehydrated in ascending grades of alcohol, sputter-coated with gold and visualized using SEM (JSM-840, JEOL, Tokyo, Japan).

Statistical analysis

Data are shown as the mean ± s.d. of a representative point from repeated experiments. Statistical analysis of the data was performed using Student's *t*-test or one-way analysis of variance. A value of $P<0.05$ was considered significant (computed by the SPSS version 19.0 software, IBM, New York, NY, USA).

RESULTS

Optical transmittance of the blended membranes

The optical transmittances of these membranes at wavelengths ranging from 400 to 800 nm were measured and the results are shown in Table 1. The transparency of the membranes was ⩾80% at the tested visible wavelengths. Previous studies demonstrated that, in these spectral regions (at 450, 500, 550, 600 and 650 nm), light transmission values of human corneas increased from 50% to 75%.[24] According to this data, the blended membranes were more transparent than human corneas. The results indicated that optical transmittance of the blended membranes could meet the requirement for CEC carriers.

Cytotoxicity evaluation of the blend membranes

The cell growth of L929 in the blend membrane extract is shown in Table 2. The results indicated that RGR in both the CMCT and CMCTS experimental groups was between 88% and 98%. According to the evaluation criterion GB/T16886.5-2003, cytotoxicity of the blended membrane extract was of scoring 1 and qualified.

Evaluation of histocompatibility and degradability in vivo

General observation of the blended membranes in subcutaneous tissues. We investigated the degradability of the CMCTS/gel and CMCT/gel blended membranes *in vivo* by implanting them into the subcutaneous tissue and skeletal muscle of rats. The animals were killed at 1, 2, 4 and 8 weeks after implantation to remove tissue specimens. The membranes in the subcutaneous tissue could be observed by the naked eye before surgery for removing the samples. As shown in Figure 1, larger fibrous encapsulations were formed around the implants of the CMCTS group compared with those of the CMCT and the suture groups at 1 week postimplantation. At 2 weeks postimplantation, there was no macroscopic fibrous encapsulation in any implant group. In addition, the CMCTS/gel membranes could be detected in the subcutaneous tissues until the eighth week, whereas the CMCT/gel membrane could only be observed in the first 4 weeks after implantation. In the control groups, the sutures did not degrade until the eighth week, and nothing was found in the sham operation and blank groups.

Table 1 Optical transmittance of the membranes

	T *of the blended membranes (%, mean ± s.d.)*	
Wavelength (nm)	*CMCTS*	*CMCT*
400	85.17 ± 0.68	82.26 ± 0.50
500	89.67 ± 0.46	88.03 ± 0.26
600	90.47 ± 0.38	89.24 ± 0.27
700	90.82 ± 0.35	89.90 ± 0.24
800	90.67 ± 0.39	89.98 ± 0.31

Abbreviations: CMCT, carboxymethyl chitin; CMCTS, carboxymethyl chitosan.
Each point represents the mean ± s.d. of five experiments.

HE staining of the blended membranes in subcutaneous tissues. Histological examination was used to observe microscopic changes of the subcutaneous tissues around the implanted membranes using HE staining. The result was consistent with the general observations. There were remarkable differences between CMCTS and CMCT blended membranes (shown by arrows in Figure 2) in terms of biodegradability in the subcutaneous tissue. The CMCTS/gel membrane was found in the subcutaneous tissues until the eighth week, whereas the CMCT/gel membrane was observed only in the first 4 weeks. As shown in Figure 2, both the implanted CMCTS/gel and CMCT/gel membranes showed degradation at 4 weeks compared with their homogeneous appearance at 1 and 2 weeks. In the negative control group, the suture showed no degradation until the eighth week. In the sham operation group, only the wound area was observed compared with the blank control.

By HE staining, numerous leukocytes were detected in the subcutaneous tissues around the two blended membranes at 1 week after the implantation surgery (Figure 2). The CMCTS/gel membranes appeared to show a more severe immune response than the CMCT/gel membranes. However, a significant decrease in the inflammatory reaction in both experimental groups was observed after the second week. In the control groups, the immune response of the suture group was similar to that of the CMCT membrane group in the first week, which was observed till week 8. There was no obvious immune reaction in the sham operation and blank groups.

HE staining of the blended membranes in the skeletal muscle. Microscopic changes of the muscle around the implanted membranes were observed using HE staining. Remarkable differences between the CMCTS/gel and CMCT/gel blended membranes (shown by arrows in Figure 3) in terms of biodegradability were observed in the skeletal muscle of rats. The CMCTS/gel membranes were detected by HE staining at 4 weeks, whereas the CMCT/gel membrane was detected only in the first 2 weeks. Neither of the embedded blended membranes was detected in the muscle tissues at 8 weeks, and the CMCT/gel membrane appeared to have cracked after the first week. In the control groups, the suture showed no degradability until the eighth week, and in the sham operation group, only the wound area was observed compared with the blank group. Overall, the blended membranes implanted in the skeletal muscles showed faster degradation rate than those in subcutaneous tissues.

Numerous leukocytes were detected in the muscles around the two kinds of embedded membranes after 1 week (Figure 3). Similar to the subcutaneous tissues, the CMCTS/gel membranes showed more severe inflammatory reaction than the CMCT/gel membranes, with an obvious decrease in response in both the experimental groups after the second week. The immune response of the suture group was similar to that of the CMCT membrane group in the first week and disappeared in the eighth week. There was no obvious immune reaction in the sham operation and blank groups.

Immunohistochemical staining. LCA is the common antigen of leukocytes. The results of immunohistochemical staining were in accordance to HE staining. As shown in Figure 4, the CMCTS/gel membranes showed more severe inflammatory reaction than the CMCT/gel membranes both in the subcutaneous and skeletal muscles

tissues. And the inflammatory reaction decreased obviously in both the experimental groups after the second week when time went on.

Liver, kidney and spleen index and histological observation. The index of liver, kidney and spleen at 1, 2, 4 and 8 weeks after implantation were calculated to explore the toxic effect of the scaffolds. As shown in Figure 5a, neither the CMCTS/gel nor the CMCT/gel membranes showed any statistically significant effect on the relative weight of these organs during 8 weeks *in vivo* compared with the blank group ($P > 0.05$). The tissue structure of the liver, kidney and spleen at 8 weeks after implantation was observed by HE staining. In Figure 5b, neither the CMCTS/gel nor the CMCT/gel membranes showed any significant effect on the tissue structure of these organs at 8 weeks *in vivo*. Thus both membranes did not influence the normal weights or tissues structure of the liver, kidney and spleen and were relatively safe for use as *in vivo* cell scaffold transplantation.

Table 2 Cytotoxicity ranking of the CMCT and CMCTS blend membranes

Group	*Absorbance*	*RGR (%)*	*Toxicity ranking*
Control—24 h	0.2689 ± 0.0159		
CMCT—24 h	0.2552 ± 0.0187	93.3	1
CMCTS—24 h	0.2575 ± 0.0127	92.6	1
Control—48 h	0.4133 ± 0.0162		
CMCT—48 h	0.3820 ± 0.0178	94.1	1
CMCTS—48 h	0.3991 ± 0.0159	95.1	1

Abbreviations: CMCT, carboxymethyl chitin; CMCTS, carboxymethyl chitosan; RGR, relative growth rate.
Each point represents the mean ± s.d. of five experiments.

Membranes as potential scaffold for CECs

Morphology and growth of CECs cultured on membranes. The growth of primary rabbit CECs in the cell culture dish is shown in Figure 6a. The Descemet's membrane was covered with CECs at 0 h (Figure 6a1), and the cells migrated from the tissue block within 24 h (Figure 6a2). To investigate the cytocompatibility of the scaffolds, rabbit CECs were cultured on the CMCTS and CMCT blended membranes. Figure 6 shows the micrographs of the CECs spread on the membrane surface after 48 h of culture. Cell adhesion and growth were observed using light and fluorescence microscopy (Figure 6b). Cell adhesion and morphology could not be observed clearly using light microscopy. After CFSE fluorescent staining, a large number of CECs were observed to have reached confluence with a cobble-stone appearance. The results showed that the cells reached confluence and maintained their normal morphology and adhesion activity in both blended membranes. The viability of the CECs was detected quantitatively using the MTT assay at 24 and 48 h (Figure 6c). There was no

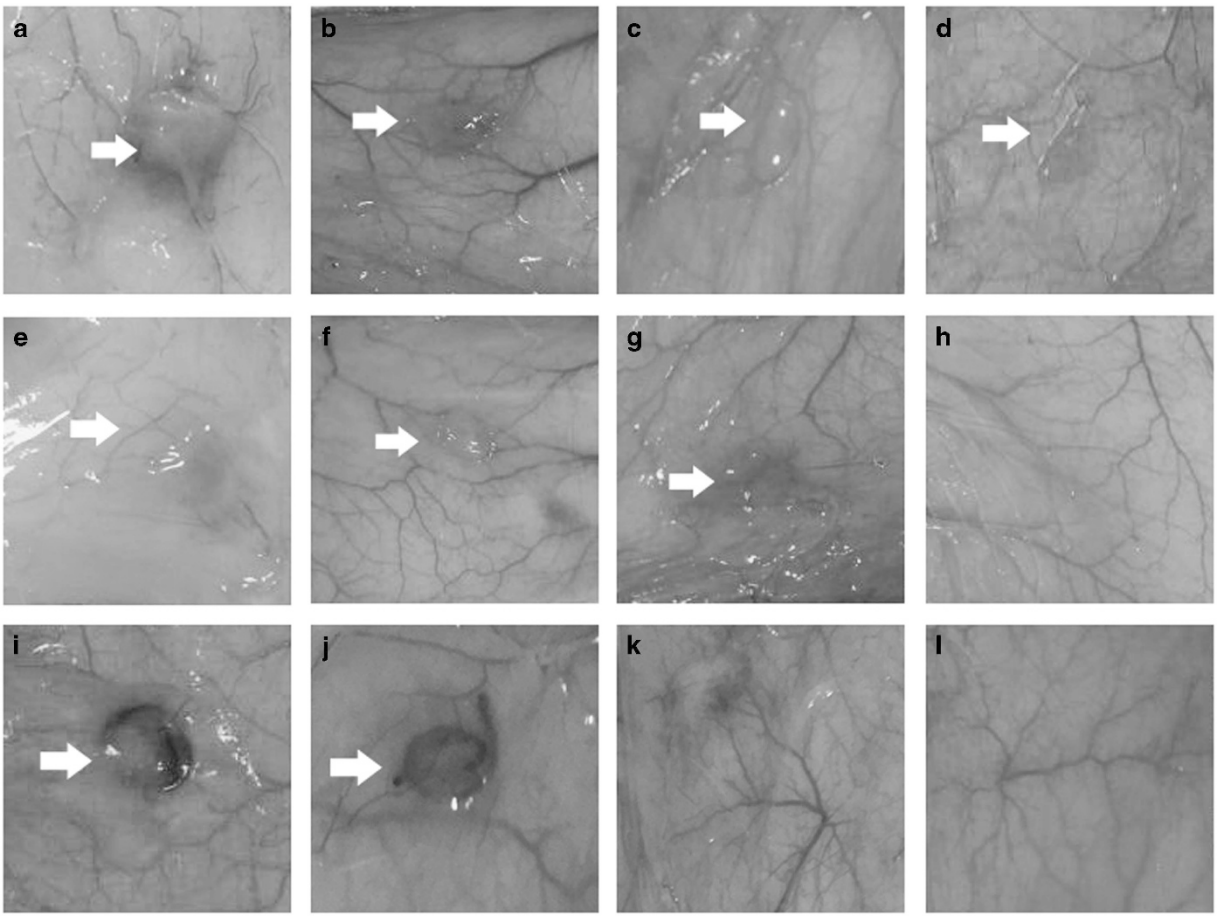

Figure 1 General observations of the carboxymethyl chitosan (CMCTS) (**a**–**d**) and carboxymethyl chitin (CMCT) (**e**–**h**) blended membranes in subcutaneous tissues at 1, 2, 4 and 8 weeks after implantation, respectively. The sutures in the subcutaneous tissues at 1 and 8 weeks are shown in (**i**, **j**), while the sham operation and control groups shown in (**k**, **l**), respectively. An arrow indicates the implanted membranes or sutures in the subcutaneous tissues. A full color version of this figure is available at the *Polymer Journal* online.

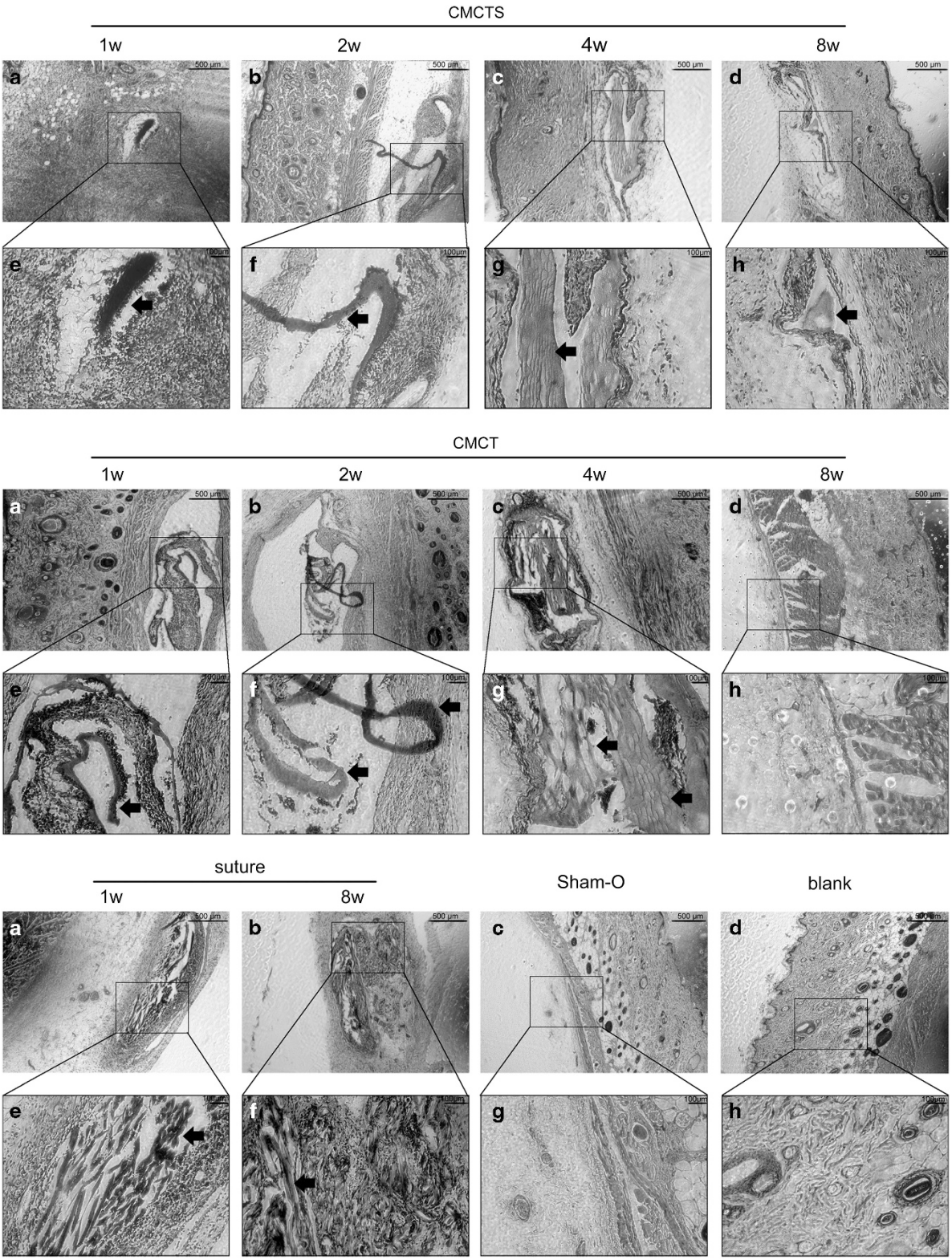

Figure 2 Histological section photomicrographs of the subcutaneous tissues around the carboxymethyl chitosan (CMCTS) and carboxymethyl chitin (CMCT) implanted membranes, suture and blank groups under light microscopy (×40). The membranes, sutures, wounds or normal areas are magnified in the box. An arrow indicates the implanted membranes (in the experiment groups) or sutures (in the negative control group) in the subcutaneous tissues. A full color version of this figure is available at the *Polymer Journal* online.

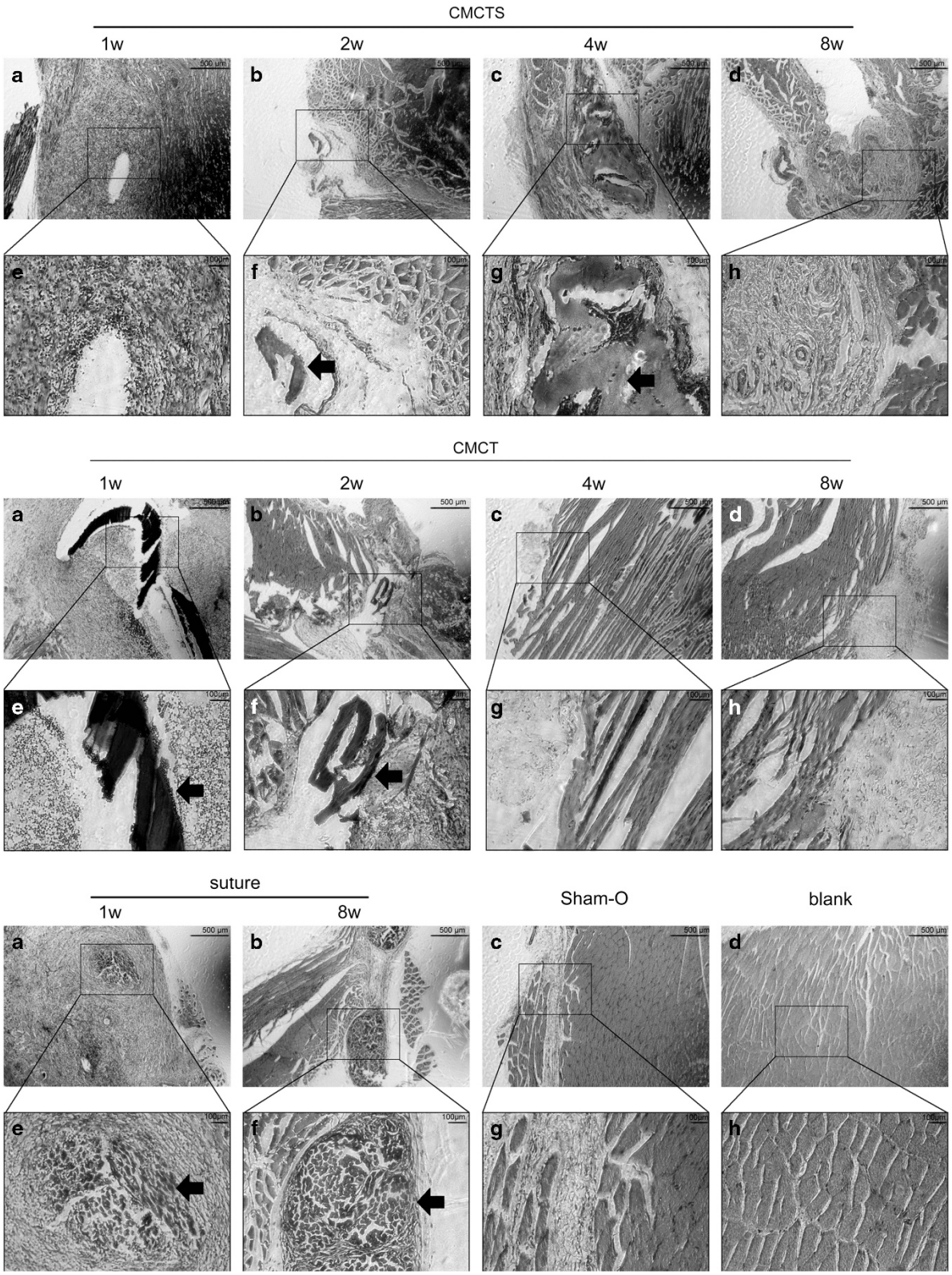

Figure 3 Histological section photomicrographs of the muscle around the carboxymethyl chitosan (CMCTS) and carboxymethyl chitin (CMCT) implanted membranes, sutures and blank groups under light microscopy (×40). The membranes, sutures, wounds or normal areas are magnified in the box. An arrow indicates the implanted membranes or sutures in the muscle tissues. A full color version of this figure is available at the *Polymer Journal* online.

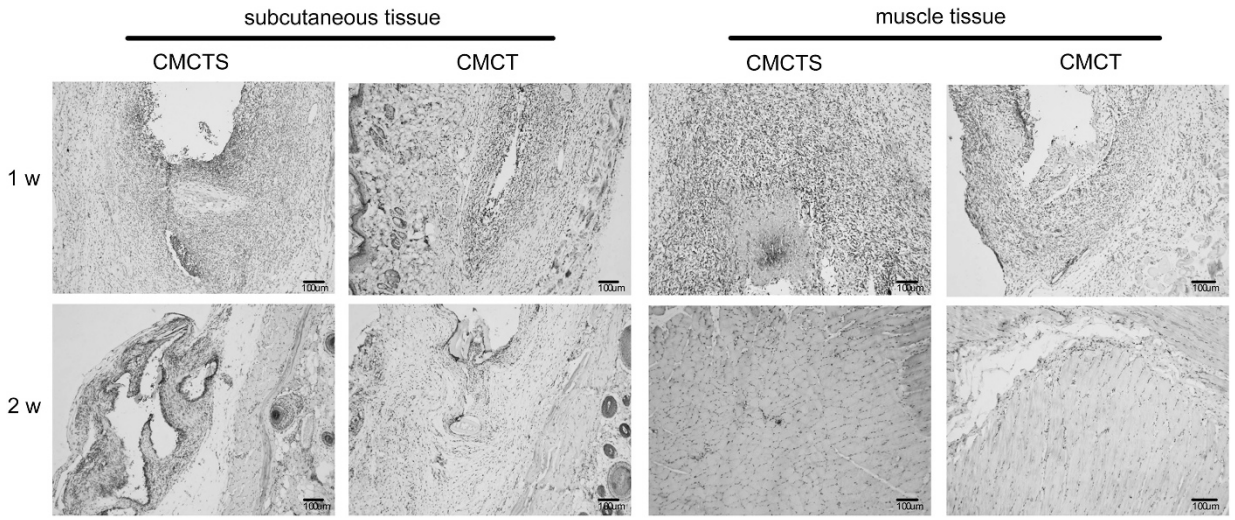

Figure 4 Immumohistochemical staining of subcutaneous and skeletal muscle tissues around the implanted blended membranes at 1 and 2 weeks after the surgery. A full color version of this figure is available at the *Polymer Journal* online.

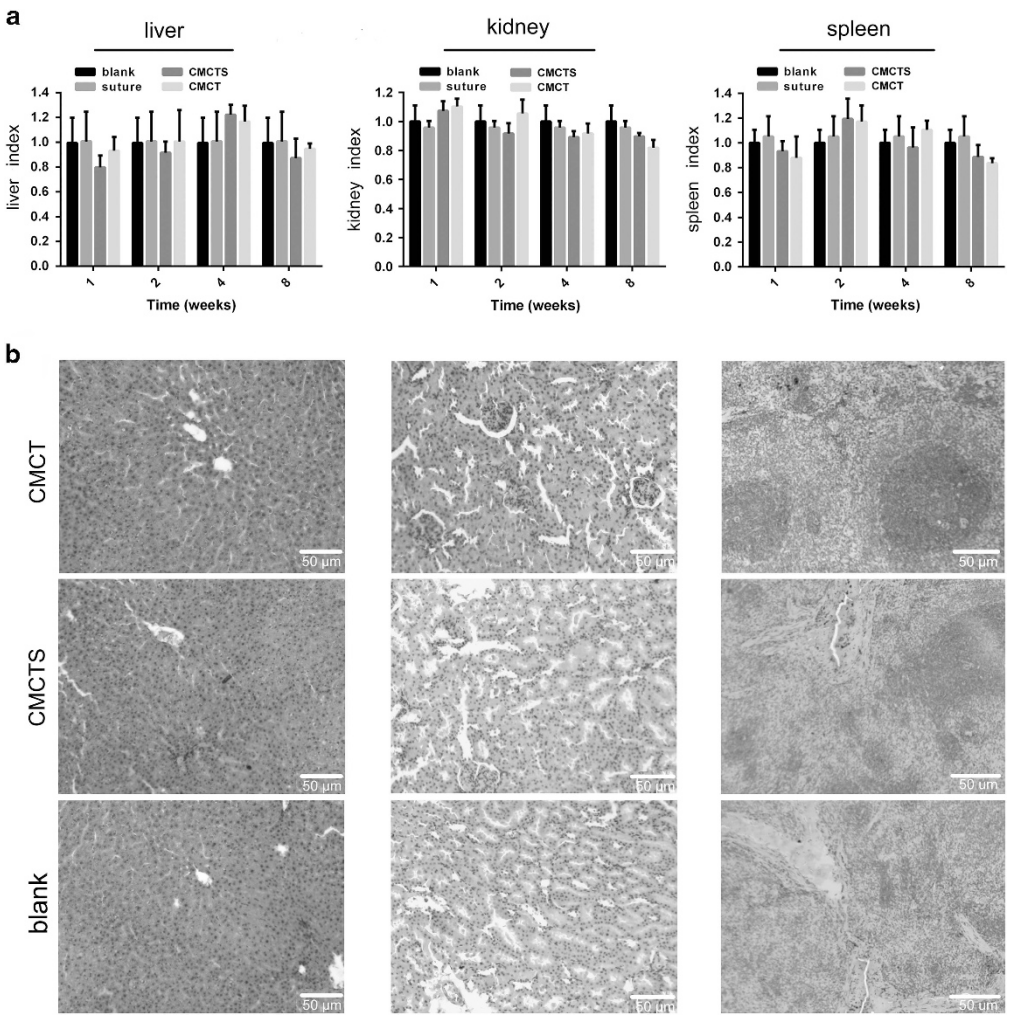

Figure 5 Relative weight (**a**) and histological observation (**b**) of the liver, kidney and spleen of laboratory animals. Both the carboxymethyl chitosan (CMCTS)/gelatin and carboxymethyl chitin (CMCT)/gelatin groups showed no significant effect on the relative weight or tissue structure of these organs during 8 weeks. A full color version of this figure is available at the *Polymer Journal* online.

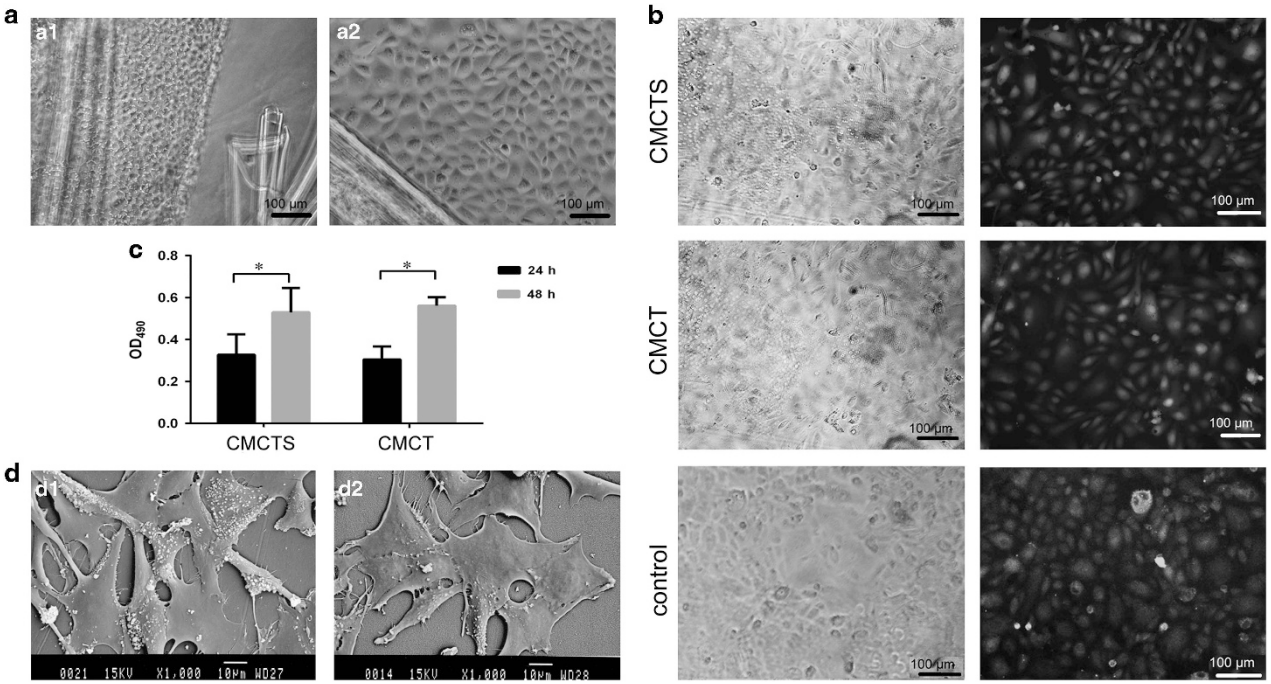

Figure 6 Micrographs of primary rabbit corneal endothelial cells (CECs) obtained by the tissue block method at 0 h (a1) and 24 h (a2) and the CECs spread on the carboxymethyl chitosan (CMCTS) and carboxymethyl chitin (CMCT) blended membranes and cell cultured plate after culture for 2 days observed by light microscopy (×100) and fluorescence microscopy (×100) (**b**). Analysis of the OD_{490} values (**c**) for CECs cultured on the blended membranes for 72 h shows no statistically significant difference between the two blended membranes ($P>0.05$). Asterisk denotes significant differences of OD_{490} values in both the CMCTS and CMCT groups at 48 h compared with that at 24 h ($P<0.05$) as determined by the Student's *t*-test. CECs cultured on CMCTS (d1) and CMCT (d2) membranes were detected by scanning electron microscopy (SEM) (×1000). A full color version of this figure is available at the *Polymer Journal* online.

statistically significant difference in cell proliferation between the CMCTS and CMCT blended membranes ($P>0.05$) at the same time. However, there were significant differences of OD_{490} values in both the CMCTS and CMCT groups at 48 h compared with that at 24 h ($P<0.05$), which showed that CECs could grow on the two membranes.

SEM of CECs cultured on membranes. The CECs cultured on the membranes were observed using SEM on the second day. Cohesive cell organization and abundant microvillion on the surface of the spread cells were observed (Figures 6d1 and d2), which indicated that the attachment and exchange functions among consecutive cells were similar to those of native CEC.[25] Therefore, the results suggested that the blended membranes had good cytocompatibility.

DISCUSSION

Recently, corneal tissue engineering has evolved dramatically from *in vitro* cell culture to generation of biomedical scaffolds for artificial corneas using materials such as the Descemet's membrane,[26] amniotic membrane,[27] thin gel membranes,[28] collagen sheets,[5] silk fibroin membranes and different synthetic polymers. Although these carriers have good biocompatibility, they cause complications after transplantation into the corneal stroma.[29] Therefore, despite the significant progress in engineered corneal replacements, problems persist that require further improvement and research.

Naturally derived polymers have received much attention in medical materials science and biotechnology for their distinct biocompatible properties. Several studies have focused on chitosan or chitin-based materials as corneal endothelial carriers. Young *et al.*[30] examined the proliferative abilities, phenotypic expressions and extracellular matrix protein production of bovine CECs seeded on chitosan/polycaprolactone blended membranes. The results suggested the membranes to be an optimized biomaterial for the fabrication of bioengineered corneal endothelium. Liang *et al.*[21] demonstrated that membranes composed of hydroxyethyl chitosan, gel and chondroitin sulfate had superior transparency, equilibrium water content, ion and glucose permeability and biocompatibility as CEC carrier. CMCTS and CMCT are water-soluble derivatives of chitosan and chitin that possess excellent properties. However, few studies have focused on the use of CMCTS or CMCT composites in corneal endothelium transplantation. Studies on the different properties of these biomaterials are limited. In our study, CMCT and CMCTS blended membranes with good mechanical strength and flexibility were selected as trial corneal endothelial carriers.

The transparency of the implanted membranes is a critical indicator of the quality of corneal transplantation. Implanted chitosan or chitin-based materials have good transmittance. Gao *et al.*[31] demonstrated that the transmittance of the hydroxypropyl chitosan membrane ranged from 90% to 97%. Chen *et al.*[32] determined the transmittance of collagen/chitosan blended membrane to be 78–95%. In the present study, the optical transmittance of the membranes in the wavelength range of 400–800 nm ranged from 82% to 91%. The transmittance was higher compared with that of human corneas, which suggested that both CMCTS/gel and CMCT/gel blended membranes were suitable as corneal endothelial scaffolds in terms of transparency.

Chitin and chitosan are both depolymerized predominantly by lysozyme, a muramidase that is distributed widely in human tissues. However, the details of the degradation mechanism of chitin and chitosan (and their derivatives) *in vivo* are unclear, and there may be underlying mechanisms that increase their degradation over time. Generally, the rate and extent of degradation of materials are related to

the average molecular weight and the degree of deacetylation. Compounds with lower molecular weight and degree of deacetylation are more susceptible,[33] possibly because lysozyme targets acetylated residues.[34] Several studies have been performed on the degradability of chitin or chitosan-based implant materials *in vitro* and *in vivo*.[15,35] However, chitin and chitosan occur in variety of forms that differ in size and degree of deacetylation, and numerous chemical modifications increase this diversity exponentially.[36,37] As the derivatives may possess markedly different characteristics compared with their parent material, further studies on their degradability and elicited immune responses are still required.

In our study, the two types of membranes implanted in the subcutaneous tissue and skeletal muscle of rat showed remarkable differences in biodegradability. In subcutaneous tissues, the CMCTS/gel membrane persisted until week 8, whereas the CMCT/gel membrane was only observed in the first 4 weeks. HE staining showed that the implanted CMCTS/gel and CMCT/gel membranes were degraded after 4 weeks compared with their homogeneous appearance at 1 and 2 weeks postimplantation. In the skeletal muscles, the CMCTS/gel membranes could still be detected at 4 weeks, while the CMCT/gel membrane was only observed in the first 2 weeks after implantation. Both the embedded blended membranes disappeared after 8 weeks. Thus the CMCT/gel membrane degraded faster than the CMCTS/gel membrane in the subcutaneous tissue and skeletal muscle, which might be related to its higher acetylation. Moreover, the blended membranes implanted in the skeletal muscles degraded faster than those embedded in subcutaneous tissues, possibly because of increased fluids and enzymes in the former.

The immune response to the blended membranes is another important aspect in the application of CMCTS and CMCT in tissue engineering.[20] During the degradation process, the scaffold might induce immune cell stimulation and local cell proliferation, ultimately affecting integration of the implanted material with the host tissue.[38] At the first week after implantation, numerous neutrophils were observed in both the subcutaneous and muscle tissues around the two blended membranes; however, this inflammatory reaction reduced significantly after the second week in both the experimental groups. The immune response might be ascribed to the availability of amino groups to immunocytes[39]; however, there was no continuous rejection of the extraneous membranes during degradation. The CMCTS/gel membranes showed a more severe immune response than the CMCT/gel membranes in subcutaneous and muscle tissues. Therefore, the results suggested that the CMCT/gel membranes possessed lower immunogenicity and might be a promising cell scaffold for tissue engineering.

Although there appears to be much potential for the application of both CMCTS and CMCT as scaffolds for tissue transplantation, more attention should be focused on the toxicity of the biomaterials *in vivo*, especially during their degradation. In our study, the relative weights of the liver, kidney and spleen after the implantation showed no significant differences among the groups, which indicated that both the CMCTS/gel and CMCT/gel membranes were nontoxic and relatively safe for use in cell scaffold transplantation *in vivo*.

CECs, especially human CECs, have limited proliferation rates because they are arrested in the G1 phase.[40,41] Therefore, researchers are actively seeking to replace the corneal endothelium through cell culture and tissue engineering-based techniques. Cell death and poor initial vitality of CECs are assumed to be responsible for the majority of corneal transplant failures.[42] In both the CMCT and CMCTS membrane groups, viable CECs could attach tightly on the surface of the blended membranes with numerous microvilli, as observed using SEM, which indicated that the attachment and exchange among consecutive cells was similar to those of native CECs.[43] The MTT assay showed that there was no statistically significant difference in cell viability between the CMCTS and CMCT membrane groups ($P > 0.05$). Thus both the CMCTS/gel and CMCT/gel blended membranes showed similar cytocompatibilities. In both the CMCTS and CMCT membrane groups, the OD_{490} values at 48 h were higher than those at 24 h. This showed that both membranes supported the proliferation of CECs.

Considering these characteristics, materials based on CMCT could be attractive candidates for future use in CEC scaffold tissue regeneration. To date, however, attention has been paid to chitosan and its derivative-based biomaterials in other diverse applications. However, importantly, chitin and its derivatives possess inherently favorable material and chemical properties. Nonetheless, the development of an ideal biomedical scaffold for tissue engineering remains a challenge.

CONCLUSIONS

In our study, corneal endothelial scaffolds were prepared successfully with CMCTS or CMCT blended with gel at a mass ratio of 20:1. Both the CMCTS/gel and CMCT/gel blended membranes exhibited good transparency, cytocompatibility and relatively low toxicity. However, the CMCT/gel membranes showed a higher degradation rate *in vivo* and a milder immune response compared with the CMCTS/gel membrane. Thus the CMCT/gel blended membrane is a more promising candidate for constructing CEC endothelial scaffold for corneal replacement.

CONFLICT OF INTEREST

The authors declare no conflict of interest.

ACKNOWLEDGEMENTS

This study was supported financially by the National Natural Science Foundations of China (81401899), the Science and Technology Development Foundation of Shandong Province (2014GHY115025), the Natural Science Foundation of Shandong Province (ZR2014HP011), the Qingdao Young Scientist Applied Basic Research fund (15-9-1-51-jch) and the National Nature Science Foundation of China (81770900).

1 Ljubimov, A. & Saghizadeh, M. Progress in corneal wound healing. *Prog. Retin. Eye Res.* **49**, 17–45 (2015).
2 Joyce, N. C. Proliferative capacity of corneal endothelial cells. *Exp. Eye Res.* **95**, 16–23 (2012).
3 Pineda, R. Corneal transplantation in the developing world: lessons learned and meeting the challenge. *Cornea* **10**, S35–S40 (2015).
4 Gain, P., Jullienne, R., He, Z., Aldossary, M., Acquart, S., Cognasse, F. & Thuret, G. Global survey of corneal transplantation and eye banking. *JAMA Ophthalmol.* **134**, 167–173 (2016).
5 Mimura, T., Yamagami, S., Yokoo, S., Usui, T., Tanaka, K., Hattori, S., Irie, S., Miyata, K., Araie, M. & Amano, S. Cultured human corneal endothelial cell transplantation with a collagen sheet in a rabbit model. *Invest. Ophthalmol. Vis. Sci.* **45**, 2992–2997 (2004).
6 Honda, N., Mimura, T., Usui, T. & Amano, S. Descemet stripping automated endothelial keratoplasty using cultured corneal endothelial cells in a rabbit model. *Arch. Ophthalmol.* **127**, 1321–1326 (2009).
7 Joo, C. K., Green, W. R., Pepose, J. S. & Fleming, T. P. Repopulation of denuded murine Descemet's membrane with life-extended murine corneal endothelial cells as a model for corneal cell transplantation. *Graefes Arch. Clin. Exp. Ophthalmol.* **238**, 174–180 (2000).
8 Lai, J., Chen, K. & Hsiue, G. Tissue-engineered human corneal endothelial cell sheet transplantation in a rabbit model using functional biomaterials. *Transplantation* **84**, 1222–1232 (2007).
9 Yang, Y., Yang, S., Wang, Y., Yu, Z., Ao, H., Zhang, H., Qin, L., Guillaume, O., Eglin, D., Richards, R. G. & Tang, T. Anti-infective efficacy, cytocompatibility and biocompatibility of a 3D-printed osteoconductive composite scaffold functionalized with quaternized chitosan. *Acta Biomater.* **46**, 112–128 (2016).

10 Muzzarelli, R., Baldassarre, V., Conti, F., Ferrara, P., Biagini, G., Gazzanelli, G. & Vasi, V. Biological activity of chitosan: ultrastructural study. *Biomaterials* **9**, 247–252 (1988).
11 Chen, X., Wang, Z., Liu, W. & Park, H. The effect of carboxymethyl-chitosan on proliferation and collagen secretion of normal and keloid skin fibroblasts. *Biomaterials* **23**, 4609–4614 (2002).
12 Jain, A., Gulbake, A., Shilpi, S., Jain, A., Hurkat, P. & Jain, S. A new horizon in modifications of chitosan: syntheses and applications. *Crit. Rev. Ther. Drug* **30**, 91–181 (2013).
13 Chen, S., Wu, Y., Mi, F., Lin, Y., Yu, L. & Sung, H. A novel pH-sensitive hydrogel composed of N,O-carboxymethyl chitosan and alginate cross-linked by genipin for protein drug delivery. *J. Control. Release* **96**, 285–300 (2004).
14 Yu, S., Zhang, X., Tan, G., Tian, L., Liu, D., Liu, Y., Yang, X. & Pan, W. A novel pH-induced thermosensitive hydrogel composed of carboxymethyl chitosan and poloxamer cross-linked by glutaraldehyde for ophthalmic drug delivery. *Carbohyd. Polym.* **155**, 208–217 (2017).
15 Liu, Z., Wang, C., Liu, Y. & Peng, D. Cefepime loaded O-carboxymethyl chitosan microspheres with sustained bactericidal activity and enhanced biocompatibility. *J. Biomat. Sci. Polym. Ed.* **28**, 79–92 (2017).
16 Upadhyaya, L., Singh, J., Agarwal, V. & Tewari, R. The implications of recent advances in carboxymethyl chitosan based targeted drug delivery and tissue engineering applications. *J. Control. Release* **186**, 54–87 (2014).
17 Wang, Y., Van, Manh, N., Wang, H., Zhong, X., Zhang, X. & Li, C. Synergistic intrafibrillar/extrafibrillar mineralization of collagen scaffolds based on a biomimetic strategy to promote the regeneration of bone defects. *Int. J. Nanomed.* **11**, 2053–2067 (2016).
18 Fan, M., Ma, Y., Tan, H., Jia, Y., Zou, S., Guo, S., Zhao, M., Huang, H., Ling, Z., Chen, Y. & Hu, X. Covalent and injectable chitosan-chondroitin sulfate hydrogels embedded with chitosan microspheres for drug delivery and tissue engineering. *Mat. Sci. Eng. C Mater. Biol. Appl.* **71**, 67–74 (2017).
19 Liu, W., Li, S., Chang, J., Han, B. & Liu, W. Preparation and physicochemical property of carboxymethyl-chitosan/hyaluronic acid poly(vinyl alcohol) blend membrane. *Zhongguo Xiu Fu Chong Jian Wai Ke Za Zhi* **23**, 1012–1016 (2009).
20 Wan, A. & Tai, B. CHITIN–a promising biomaterial for tissue engineering and stem cell technologies. *Biotechnol. Adv.* **31**, 1776–1785 (2013).
21 Liang, Y., Liu, W. S., Han, B. Q., Yang, C. Z., Ma, Q., Zhao, W. W., Rong, M. & Li, H. Fabrication and characters of a corneal endothelial cells scaffold based on chitosan. *J. Mater. Sci. Mater. Med.* **22**, 175–183 (2011).
22 Zhu, W., Guo, W., Chen, Y., Xiu, W., Wang, D., Huang, J., Huang, J., Lu, W., Peng, L., Chen, K. & Zeng, Y. Cytocompatibility of PLA/Nano-HA composites for interface fixation. *Artif. Cells Nanomed. Biotechnol.* **44**, 1122–1126 (2016).
23 Lai, J., Cheng, H. & Ma, D. Investigation of overrun-processed porous hyaluronic acid carriers in corneal endothelial tissue engineering. *PLoS ONE* **10**, e0136067 (2015).
24 Liang, Y., Liu, W., Han, B., Yang, C., Ma, Q., Zhao, W., Rong, M. & Li, H. Fabrication and characters of a corneal endothelial cells scaffold based on chitosan. *J. Mater. Sci. Mater. Med.* **22**, 175–183 (2011).
25 Mimura, T., Yamagami, S. & Amano, S. Corneal endothelial regeneration and tissue engineering. *Prog. Retin. Eye Res.* **35**, 1–17 (2013).
26 Amano, S. Transplantation of cultured human corneal endothelial cells. *Cornea* **22**, S66–S74 (2003).
27 Watanabe, R., Hayashi, R., Kimura, Y., Tanaka, Y., Kageyama, T., Hara, S., Tabata, Y. & Nishida, K. A novel gelatin hydrogel carrier sheet for corneal endothelial transplantation. *Tissue Eng. Part A* **17**, 2213–2219 (2011).
28 Choi, J., Williams, J., Greven, M., Walter, K., Laber, P., Khang, G. & Soker, S. Bioengineering endothelialized neo-corneas using donor-derived corneal endothelial cells and decellularized corneal stroma. *Biomaterials* **31**, 6738–6745 (2010).
29 Xu, Y. Tissue-engineered membrane based on chitosan for repair of mechanically damaged corneal epithelium. *J. Mater. Sci. Mater. Med.* **25**, 2163–2171 (2014).
30 Young, T. H., Wang, I. J., Hu, F. R. & Wang, T. J. Fabrication of a bioengineered corneal endothelial cell sheet using chitosan/polycaprolactone blend membranes. *Colloid Surf. B Biointerfaces* **116**, 403–410 (2014).
31 Gao, X., Liu, W., Han, B., Wei, X. & Yang, C. Preparation and properties of a chitosan-based carrier of corneal endothelial cells. *J. Mater. Sci. Mater. Med.* **19**, 3611–3619 (2008).
32 Chen, J. S., Li, Q. H., Xu, J. T., Huang, Y. X., Ding, Y., Deng, H. W., Zhao, S. B. & Chen, R. Study on biocompatibility of complexes of collagen-chitosan-sodium hyaluronate and cornea. *Artif. Organs* **29**, 104–113 (2005).
33 Kean, T. & Thanou, M. Biodegradation, biodistribution and toxicity of chitosan. *Adv. Drug Deliv. Res.* **62**, 3–11 (2010).
34 Kim, I., Seo, S., Moon, H., Yoo, M., Park, I., Kim, B. & Cho, C. Chitosan and its derivatives for tissue engineering applications. *Biotechnol. Adv.* **26**, 1–21 (2008).
35 Rahmani, S., Mohammadi, Z., Amini, M., Isaei, E., Taheritarigh, S., RafieeTehrani, N. & RafieeTehrani, M. Methylated 4-N,N dimethyl aminobenzyl N,O-carboxymethyl chitosan as a new chitosan derivative: synthesis, characterization, cytotoxicity and antibacterial activity. *Carbohydr. Polym.* **149**, 131–139 (2016).
36 Song, L., Li, L., He, T., Wang, N., Yang, S., Yang, X., Zeng, Y., Zhang, W., Yang, L., Wu, Q. & Gong, C. Peritoneal adhesion prevention with a biodegradable and injectable N,O-carboxymethyl chitosan-aldehyde hyaluronic acid hydrogel in a rat repeated-injury model. *Sci. Rep.* **6**, 37600 (2016).
37 Engelsman, A., van der Mei, H., Francis, K., Busscher, H., Ploeg, R. & van Dam, G. Real time noninvasive monitoring of contaminating bacteria in a soft tissue implant infection model. *J. Biomed. Mater. Res. B* **88**, 123–129 (2009).
38 Suh, J. & Matthew, H. Application of chitosan-based polysaccharide biomaterials in cartilage tissue engineering: a review. *Biomaterials* **21**, 2589–2598 (2000).
39 Nishimura, S., Nishi, N., Tokura, S., Nishimura, K. & Azuma, I. Bioactive chitin derivatives: activation of mouse-peritoneal macrophages by O-(carboxymethyl)chitins. *Carbohyd. Res.* **146**, 251–258 (1986).
40 Joyce, N., Meklir, B., Joyce, S. & Zieske, J. Cell cycle protein expression and proliferative status in human corneal cells. *Invest. Ophthalmol. Vis. Sci.* **37**, 645–655 (1996).
41 Vazquez, N., Chacon, M., Rodriguez-Barrientos, C., Merayo-Lloves, J., Naveiras, M., Baamonde, B., Alfonso, J., Zambrano-Andazol, I., Riestra, A. & Meana, A. Human bone derived collagen for the development of an artificial corneal endothelial graft: in vivo results in a rabbit model. *PLoS ONE* **11**, e0167578 (2016).
42 Bandela, P., Satgunam, P., Garg, P. & Bharadwaj, S. Corneal transplantation in disease affecting only one eye: does it make a difference to habitual binocular viewing? *PLoS ONE* **11**, e0150118 (2016).
43 Khor, E. & Lim, L. Implantable applications of chitin and chitosan. *Biomaterials* **24**, 2339–2349 (2003).